8-2010

Propagation of Periodic Waves Using Wave Confinement

Paula Cysneiros Sanematsu
University of Tennessee - Knoxville, psanemat@utk.edu

To the Graduate Council:

I am submitting herewith a thesis written by Paula Cysneiros Sanematsu entitled "Propagation of Periodic Waves Using Wave Confinement." I have examined the final electronic copy of this thesis for form and content and recommend that it be accepted in partial fulfillment of the requirements for the degree of Master of Science, with a major in Mathematics.

K. C. Reddy, Major Professor

We have read this thesis and recommend its acceptance:

John Steinhoff, Kenneth Kimble

Accepted for the Council:
Dixie L. Thompson

Vice Provost and Dean of the Graduate School

(Original signatures are on file with official student records.)

To the Graduate Council:

I am submitting herewith a thesis written by Paula Cysneiros Sanematsu entitled "Propagation of Periodic Waves Using Wave Confinement." I have examined the final electronic copy of this thesis for form and content and recommend that it be accepted in partial fulfillment of the requirements for the degree of Master of Science, with a major in Mathematics.

K.C. Reddy, Major Professor

We have read this thesis
and recommend its acceptance:

John Steinhoff

Kenneth Kimble

Accepted for the Council:

Carolyn R. Hodges

Vice Provost and Dean of the Graduate School

(Original signatures are on file with official student records.)

Propagation of Periodic Waves Using Wave Confinement

A Thesis Presented for
The Master of Science
Degree
The University of Tennessee, Knoxville

Paula Cysneiros Sanematsu

August 2010

To Paulo and Lúcia, for their support in all aspects and for valuing education above everything else. To Flávio, for always being my foremost example. And to Tiago, who recently joined my family and is my best friend, my support and my partner.

Para Paulo e Lúcia, pelo apoio de todas as formas e por enfatizar a educação acima de qualquer coisa. Para Flávio, por sempre ser meu exemplo. E para Tiago, que recentemente juntou-se à família e é meu melhor amigo, meu apoio e meu companheiro.

Acknowledgements

This thesis would not be possible without the help and guidance from Dr. K.C. Reddy, Dr. John Steinhoff, and Dr. Subhashini B. Chitta.

I also would like to thank several UTSI students that have helped me throughout the development of this thesis: Tony Saad, Josh Batterson, Michel Akiki and Nadim Zgheib.

This work is mainly supported by the AFOSR under a contract monitored by Dr. Arje Nachman.

Abstract

This thesis studies the behavior of the Eulerian scheme, with “Wave Confinement” (WC), when propagating periodic waves. WC is a recently developed method that was derived from the scheme “vorticity confinement” used in fluid mechanics, and it efficiently solves the linear wave equation. This new method is applicable for numerous simulations such as radio wave propagation, target detection, cell phone and satellite communications.

The WC scheme adds a nonlinear term to the discrete wave equation that adds stability with negative and positive diffusion, conserves integral quantities such as total amplitude and wave speed, and it allows wave propagation over long distances with minimal numerical diffusion, which contrasts to other numerical methods where wave propagation is affected by numerical dissipation. Previous studies have shown that WC propagates short pulses/surfaces as thin nonlinear solitary waves. In this thesis, a one-dimensional (1D) periodic wave is propagated by WC using the advection and wave equations.

For the advection equation, the parameters and the initial condition (IC) used in WC are analyzed to establish for which conditions the method can be implemented. When the IC is a positive periodic wave, the converged solution consists of a series of hyperbolic secants where the number of cycles of the IC represents the number of hyperbolic secants. Waves with varying signs are analyzed by changing the wave confinement term. For this case, the converged solution is a series of positive and

negative hyperbolic secants where each hyperbolic secant is represented by half cycle of the IC.

For the wave equation, parameters and different IC's are studied to determine when WC is feasible. For positive periodic waves, the converged solution retains its sinusoidal shape and does not converge to a series of hyperbolic secants. The waves with varying signs, however, converge to a series of hyperbolic secants as seen for the advection equation.

WC is stable for various periodic waves for both advection and wave equations, which shows WC is useful for numerically propagating periodic waveforms. Convergence depends on the wave number of the IC and on the parameters (convection speed, positive diffusion, negative diffusion) used in WC.

Contents

List of Tables

List of Figures

List of Attachments

Nomenclature

Δt	Time step
ε	Negative diffusion parameter
γ	Width of hyperbolic secant
λ_c	Wave length of the cosine wave
λ_s	Wave length of the sine wave
μ	Dissipation parameter
ν	Advection speed
Φ	Harmonic mean of ϕ
ϕ	Scalar that is propagated
ψ	Inverse of ϕ
sgn	Function that determines the sign of a quantity
σ	Computed wave speed
A_T	Total Amplitude
B	Amplitude of a hyperbolic secant

c	Continuous wave speed
E	Wave confinement term
h	Spatial step
J	Maximum value of j
j	Discrete independent variable for space
m	Number of hyperbolic secants
N	Maximum value of n
n	Discrete independent variable for time
S	Positive constant added to initial condition
T	Period of sinusoidal wave

Chapter 1

Introduction

The main objective of this thesis is to implement the recently developed scheme "Wave Confinement" (WC) for the propagation of periodic waves. WC is derived from a similar method used in fluid mechanics, "Vorticity Confinement." Previous works of WC include the propagation of short pulses as solitary waves. This thesis studies the properties of WC for 1D periodic waves over long distances.

1.1 Motivation and Historical Background

The wave equation was first published in 1747 in d'Alembert (1747). Since then, great minds such as Leonhard Euler, Daniel Bernoulli, and Joseph Fourier have developed solutions of the wave equation. Analytical solutions, however, have some limitations and are not enough to solve complex problems. With the invention of the computer, numerical methods were developed to solve those problems where analytical methods are insufficient. Traditional numerical methods discretize a partial differential equation (PDE) by the use of finite differences in a way that errors are minimized. However, these methos are necessarily dissipative for stability. On the other hand, WC minimizes dissipative errors and at the same time pays attention to the essential physics of the problem by conserving integral quantities such as total amplitude and wave speed. A similar approach is also used for shock capturing methods by Lax (1973) where conservation laws are satisfied. Here, however, the shock automatically steepens due to the physics. The main feature of WC is the implementation of a simple scheme that produces physical results in a very fast time frame.

1.2 Related Methods

It is important to know the differences and limitations of other methods in order to see the advantages of WC. Other methods that simulate high frequency wave propagation include Eikonal, Green's function and Ray Tracing.

Eikonal methods provide multiple arrival times and caustics. In these cases, however, they also require complex data management which can involve the implementation of both physical and phase spaces (Osher (2008)), or multiple grids. In contrast, WC can treat these effects for short wavelength more easily than Eikonal methods. Effects featured by WC include multiple sources, reflections, scattering from surfaces and ducts, varying index of refraction, and complex topology (Chitta (2008); Steinhoff and Chitta (2009a,b,c)).

As well as Green's function methods, WC has the capability of propagating a pulse over long distances. In addition, WC also allows the propagation through different indices of refraction and inclusion of reflection, which are easily implemented because it is an Eulerian finite difference scheme (Steinhoff and Chitta (2009a,b,c)). For the Green's function method, varying index of refraction and reflections can be treated, but it is necessary to include complicated multiple integrals in order to have different indices of refraction.

Ray tracing is a Lagrangian technique that treats pulses as markers. It can include different indices of refraction through the use of ordinary differential equations (Chitta (2008)), but it may fail to be accurate in mildly heterogenous media (Rawlinson et al. (2008)) and arrival times may not be determined (Rawlinson et al. (2008); Vinje et al. (1993)). In addition, Lagrangian schemes also require complex logic to interpolate markers when the distance between them becomes larger than a predefined limit (Vinje et al. (1993)). Finally, ray tracing also fails to produce caustics (Chitta (2008); Vinje et al. (1993)). Because of the simple Eulerian grid used in WC, it is simple to implement varying index of refraction, topographic boundary conditions, geometries of scattering objects and it can also produce caustics (Chitta (2008)).

Therefore, because of the limitations of current methods and the promising uses of WC, it is important to further investigate the behavior of WC not only for pulses, but also for periodic waves.

1.3 Plan of Thesis

This thesis studies various test cases for the propagation of periodic waves using WC.

In Chapter 2, the WC scheme is analyzed for the advection equation, a simpler form of the wave equation. The formulation of the numerical scheme is presented and the solution of the WC term is described. Results for different waves – positive waves with constant and varying amplitude and waves with varying signs – are shown and constraints for the scheme's parameters are determined.

In Chapter 3, WC is implemented for the 1D wave equation. The formulation of the numerical scheme is presented as well as test cases for different waves – positive waves with constant and varying amplitude and waves with varying signs.

Finally, Chapter 4 presents a short conclusion of the cases analyzed in this thesis.

Chapter 2

Advection Equation

Eulerian numerical methods that simulate the advection equation require discretization of the term $\partial\phi/\partial x$. Central difference is well-known for being unconditionally unstable for explicit schemes (Anderson et al. (1984); Quarteroni et al. (2007)). First-order upwind difference is highly dissipative (Anderson et al. (1984); Quarteroni et al. (2007)), which may be improved by using higher-order methods (Jameson (2000, 2003)), but at the cost of more complicated schemes and much greater computational time (Jiang and Shu (1996)) and yet, it requires that the propagated pulse is spread over a moderate number of grid cells to maintain accuracy (Jameson (2000)), and still has significant dissipation after long propagation. Finally, although implicit methods are unconditionally stable, they also are complex schemes - that become even more cumbersome when extended to more dimensions -, require large computation time (Anderson et al. (1984)), and still are dissipative. Ray tracing is a Lagragian-based method that, although it accurately traces a wavefront at certain points, it also requires complex logic at every time step to allocate the markers and interpolate the markers when they separate (Vinje et al. (1993)).

The main idea of the wave confinement (WC) method is to implement a simple, Eulerian scheme with no additional logic which results in very fast computation time. The implementation of WC involves the simplest known scheme, a first order central explicit finite difference scheme, and the addition of a nonlinear term that does not alter the integral quantities of interest, provides stability and prevents the solution from dissipating.

2.1 Formulation

2.1.1 Introduction

The advection equation

$$\frac{\partial \phi}{\partial t} + c\frac{\partial \phi}{\partial x} = 0 \tag{2.1}$$

may be discretized by a first order explicit central difference scheme which is well known to be unconditionally unstable (Anderson et al. (1984); Quarteroni et al. (2007))

$$\phi_j^{n+1} = \phi_j^n - \frac{c\Delta t}{2h}\left(\phi_{j+1}^n - \phi_{j-1}^n\right), \tag{2.2}$$

where Δt and h represent time step and spatial grid length, respectively.

Wave confinement (WC) adds a nonlinear term, E_1, to Eq.(2.2) that adds stability and minimizes diffusion

$$\phi_j^{n+1} = \phi_j^n - \frac{\nu}{2}\left(\phi_{j+1}^n - \phi_{j-1}^n\right) + E_1, \tag{2.3}$$

where $\nu = c\Delta t/h$.

E_1 is defined as $E_1 = \delta_j^2 F$, where δ_j^2 is defined by $\delta_j^2 z = z_{j-1} - 2z_j + z_{j+1}$ and $F = \mu\phi - \varepsilon\,\Phi$, where $\mu\delta_j^2\phi$ represents dissipation and $\varepsilon\,\delta_j^2\Phi$ represents negative diffusion. Then Eq. (2.3) can be written as

$$\phi_j^{n+1} = \phi_j^n - \frac{\nu}{2}\left(\phi_{j+1}^n - \phi_{j-1}^n\right) + \mu\left(\phi_{j-1}^n - 2\phi_j^n + \phi_{j+1}^n\right) - \varepsilon\left(\Phi_{j-1}^n - 2\Phi_j^n + \Phi_{j+1}^n\right), \tag{2.4}$$

where $\mu = \Delta t \mu' / h^2$ and $\varepsilon = \Delta t \, \varepsilon' / h^2$. There are many possibilities for Φ_j^n. Here, it is defined as the harmonic mean of ϕ_j^n

$$\Phi_j^n = \frac{3}{\frac{1}{\phi_{j-1}^n} + \frac{1}{\phi_j^n} + \frac{1}{\phi_{j+1}^n}}. \tag{2.5}$$

The harmonic mean is chosen as the nonlinear term because it is a weighting average that weights towards the lesser value, which facilitates the convection of waves traveling in different directions.

E_1 also preserves the essential physics of Eq.(2.1) by conserving the total amplitude

$$A_T = \sum_{j=0}^{J-1} \phi_j^n, \tag{2.6}$$

where J is the total number of gridpoints in the grid.

Chitta (2008) showed that centroid speed is conserved for a single pulse. For periodic waves, however, we analyze the wave speed, which is defined by

$$\sigma = \frac{\lambda_s}{T} \tag{2.7}$$

where λ_s is the wave length and T is the period of a sinusoidal wave.

In addition, E_1 should be homogenous of order 1 to maintain the homogeneity of Eq. (2.2) (Steinhoff and Chitta (2009a)), so that $f(\alpha\phi) = \alpha f(\phi)$ for an arbitrary scalar α. When $\alpha\phi$ is propagated, the nonlinear term becomes

$$\Phi_j^n(\alpha\phi_j^n) = \frac{3}{\frac{1}{\alpha\phi_{j-1}^n} + \frac{1}{\alpha\phi_j^n} + \frac{1}{\alpha\phi_{j+1}^n}} = \alpha \frac{3}{\frac{1}{\phi_{j-1}^n} + \frac{1}{\phi_j^n} + \frac{1}{\phi_{j+1}^n}} = \alpha\Phi_j^n(\phi_j^n). \tag{2.8}$$

Since the remainder of the equation is linear, it is clear that $f(\alpha\phi) = \alpha f(\phi)$.

2.1.2 Solitary Wave Solution of Wave Confinement

Let the discrete derivative of a function $f(n)$ be

$$\Delta_n f(n) = f(n+1) - f(n). \tag{2.9}$$

Then the advection equation with WC can be written as

$$\Delta_n \phi(j,n) + c\Delta_j \phi(j,n) = \Delta_j^2 F(j,n), \tag{2.10}$$

where Δ_j^2 is the second order derivative with respect to j. And we denote

$$\phi = L(j,n). \tag{2.11}$$

Then the transformation that gives the moving frame (the frame that convects with the wave speed) is

$$\begin{aligned} \xi &= j - cn \\ \eta &= n \end{aligned} \tag{2.12}$$

which gives

$$\begin{aligned} f(\xi,\eta) &= j = \xi + c\eta \\ g(\xi,\eta) &= n = \eta. \end{aligned} \tag{2.13}$$

Let ϕ' be the transformation of ϕ using Eq. (2.13)

$$L(j,n) = \phi(j,n) = \phi'(\xi,\eta) = M(\xi,\eta). \tag{2.14}$$

Then the discrete approximation to the partial derivatives of M are

$$\begin{aligned}\Delta_\xi M &= (\Delta_j L)(\Delta_\xi f) + (\Delta_n L)(\Delta_\xi g) \\ &= (\Delta_j L)\left[(\xi + 1 + c\eta) - (\xi + c\eta)\right] + (\Delta_n L)0 \\ &= (\Delta_j L)\end{aligned} \tag{2.15}$$

$$\begin{aligned}\Delta_\eta M &= (\Delta_j L)(\Delta_\eta f) + (\Delta_n L)(\Delta_\eta g) \\ &= (\Delta_j L)\left[\xi + c(n+1) - (\xi + cn)\right] + (\Delta_n L)(\eta + 1 - \eta) \\ &= c(\Delta_j L) + \Delta_n L.\end{aligned} \tag{2.16}$$

Eq.'s (2.14) and (2.15) give

$$\Delta_j \phi(j,n) = \Delta_j L = \Delta_\xi M. \tag{2.17}$$

And Eq.'s (2.11), (2.14), (2.15), and (2.16) give

$$\Delta_n \phi(j,n) = \Delta_n L = \Delta_\eta M - c\Delta_\xi M. \tag{2.18}$$

When Eq.'s (2.17) and (2.18) are substituted into Eq. (2.10), they yield

$$\begin{aligned}\Delta_\eta M - c\Delta_\xi M + c\Delta_\xi M &= \Delta_j^2 F(j,n) \\ \Delta_\eta M &= \Delta_j^2 F(j,n)\end{aligned} \tag{2.19}$$

Now, we derive the transformation of variables for the F-term. First, define F as

$$F = F(j,n) \tag{2.20}$$

and let F' be the transformation using Eq. (2.12)

$$F(j,n) = F'(\xi,\eta) = G(\xi,\eta). \tag{2.21}$$

Then the first partial derivative of G with respect to ξ is

$$\begin{aligned}\Delta_\xi G &= (\Delta_j F)(\Delta_\xi f) + (\Delta_n F)(\Delta_\xi g) \\ &= (\Delta_j F)\left[(\xi + 1 + c\eta) - (\xi + c\eta)\right] + (\Delta_n F)0 \\ &= (\Delta_j F)\end{aligned} \tag{2.22}$$

and define

$$\Delta_j F = F_1(j, n). \tag{2.23}$$

The second partial derivative of G with respect to ξ is

$$\begin{aligned}\Delta_\xi^2 G &= (\Delta_j F_1)(\Delta_\xi f) + (\Delta_n F_1)(\Delta_\xi g) \\ &= (\Delta_j F_1)\left[(\xi + 1 + c\eta) - (\xi + c\eta)\right] + (\Delta_n F_1)0 \\ &= (\Delta_j F_1),\end{aligned} \tag{2.24}$$

where F_1 is defined by Eq. (2.23). Then, Eq. (2.24) becomes

$$\Delta_\xi^2 G = \Delta_j(\Delta_j F) = \Delta_j^2 F. \tag{2.25}$$

Finally, when Eq. (2.25) is substituted into Eq. (2.19), it yields the moving frame

$$\Delta_\eta M = \Delta_\xi^2 G. \tag{2.26}$$

At asymptotic state, $\Delta_\eta M = 0$ (with $M = 0$ at boundaries) and thus, Eq.(2.26) becomes

$$\Delta_\xi^2 G = 0, \tag{2.27}$$

or in terms of $F(j, n)$

$$\Delta_j^2 F = 0, \tag{2.28}$$

which gives

$$F_j^n = \mu\phi_j^n - \varepsilon\,\Phi_j^n = 0, \tag{2.29}$$

and

$$\mu\phi_j^n = \varepsilon\,\Phi_j^n = \frac{3\,\varepsilon}{\frac{1}{\phi_{j-1}^n} + \frac{1}{\phi_j^n} + \frac{1}{\phi_{j+1}^n}} \tag{2.30}$$

and yields the nonlinear equation

$$\mu\left(\frac{1}{\phi_{j-1}^n} + \frac{1}{\phi_j^n} + \frac{1}{\phi_{j+1}^n}\right) - \frac{3\,\varepsilon}{\phi_j^n} = 0. \tag{2.31}$$

It may be observed that Eq. (2.31) is linear in terms of $1/\phi$. Then, let

$$\psi_j^n = \frac{1}{\phi_j^n}, \tag{2.32}$$

then Eq.(2.31) becomes

$$\mu\left(\psi_{j-1}^n + \psi_j^n + \psi_{j+1}^n\right) - 3\,\varepsilon\,\psi_j^n = 0. \tag{2.33}$$

Suppose

$$\psi_j^n = e^{\gamma(j-j_0)}, \tag{2.34}$$

then

$$\mu\left(e^{\gamma(j-1-j_0)} + e^{\gamma(j-j_0)} + e^{\gamma(j+1-j_0)}\right) - 3\,\varepsilon\,e^{\gamma(j-j_0)} = 0 \tag{2.35}$$

which simply is

$$e^{-\gamma} + e^{\gamma} = \frac{3\,\varepsilon}{\mu} - 1. \tag{2.36}$$

Using the definition of the hyperbolic cosine, $2\cosh(z) \equiv e^z + e^{-z}$, Eq.(2.36) may be written as

$$2\cosh(\gamma) = \frac{3\,\varepsilon}{\mu} - 1 \tag{2.37}$$

which leads to

$$\gamma = \operatorname{arccosh}\left[\frac{1}{2}\left(\frac{3\,\varepsilon}{\mu} - 1\right)\right]. \tag{2.38}$$

Eq.(2.34) along with γ, defined by Eq.(2.38), is a solution to the linear homogeneous Eq.(2.33). Because of the symmetry in γ, it is clear that $\psi_j^n = e^{-\gamma(j-j_0)}$

is also a solution of Eq.(2.33). Then, the principle of superposition gives

$$\psi_j^n = \frac{C}{2}\left(e^{\gamma(j-j_0)} + e^{-\gamma(j-j_0)}\right) = B\cosh\left[\gamma(j-j_0)\right]. \tag{2.39}$$

Finally, using Eq.(2.32), the solution of ϕ_j^n is

$$\phi_j^n = B\,\mathrm{sech}\left[\gamma(j-j_0)\right]. \tag{2.40}$$

It is important to note that the superposition principle can be applied at the ψ_j^n level, but not at the ϕ_j^n level because Eq.(2.33) is linear whereas Eq.(2.31) is nonlinear. Even though we do not have mathematical superposition for Eq.(2.31), we do see an effective superposition of sufficiently separated hyperbolic secants as will be shown in the results and discussion section.

2.2 Positive Waves with Constant Amplitude

2.2.1 Numerical Experiment

Discretized Equation

The following discretized equation (Eq. (2.4))

$$\phi_j^{n+1} = \phi_j^n - \frac{\nu}{2}\left(\phi_{j+1}^n - \phi_{j-1}^n\right) + \mu\left(\phi_{j-1}^n - 2\phi_j^n + \phi_{j+1}^n\right) - \varepsilon\left(\Phi_{j-1}^n - 2\Phi_j^n + \Phi_{j+1}^n\right)$$

is used to perform the numerical experiments.

Boundary Conditions

Periodic boundary conditions ($\phi_0^n = \phi_{J-1}^n$)* are used for these numerical experiments.

*The right boundary is $J-1$ because if the total number of gridpoints is J and J starts at zero, then the last gridpoint is $J-1$

Initial Condition

The following initial condition is used

$$\phi_j^0 = \left[2 + \sin\left(\frac{2\pi j}{\lambda_s}\right)\right] \tag{2.41}$$

where 2 is added to ϕ_j^0 to get a positive sinusoidal wave.

2.2.2 Amplitude of Analytical Solution

The total amplitude of a hyperbolic secant is

$$\int_{-\infty}^{\infty} B \operatorname{sech}(\gamma x) dx = \frac{B\pi}{\gamma}. \tag{2.42}$$

Therefore, m hyperbolic secants have the following total amplitude

$$A_T = m\frac{B\pi}{\gamma}, \tag{2.43}$$

and the amplitude B of a single hyperbolic secant is

$$B = \frac{A_T\gamma}{m\pi}, \tag{2.44}$$

where A_T is obtained from Eq.(2.6).

2.2.3 Transformation of Converged Solution to Initial Condition

This study analyzes the behavior of a period wave by WC. To do so, we use a positive sine wave as initial condition (IC) and propagate it using WC. The exact (PDE) solution is a series of hyperbolic secants where the number of cycles of the IC represents the number of hyperbolic secants. This is also true in discretized form if the wave peaks are far enough apart so that the exponential tails have little overlap.

The number of hyperbolic secants, m, which is easily obtained by a simple logic in the program. Then, the wave length of the IC can be acquired from

$$\lambda_s = \frac{(J-1)}{m} \tag{2.45}$$

and the positive constant is

$$S = \frac{A_T}{J-1}, \tag{2.46}$$

where A_T is obtained from Eq.(2.43), which yields the following IC

$$\phi^0_{j_{\text{calculated}}} = S + \sin\left(\frac{2\pi}{\lambda_s}x\right). \tag{2.47}$$

2.2.4 Results and Discussion

Addition of Wave Confinement Term

The wave confinement (WC) method uses a first-order central difference scheme, which, by itself, is known to be unconditionally unstable (Anderson et al. (1984); Quarteroni et al. (2007)). However, as mentioned before, the addition of E adds stability, positive and negative diffusion, which allows wave propagation with no increasing numerical error. Fig. 2.1 shows how dissipative the scheme is without negative diffusion, $\varepsilon\, \delta_j^2 \Phi$.

Conservation of Physical Properties

WC is based on the conservation of some physical properties such as total amplitude, Eq. (2.6), and wave speed, Eq.(2.7).

Steinhoff and Chitta (2009a) found that for a single hyperbolic secant, the total amplitude is constant. However, for a periodic wave, the total amplitude should vary within bounded limits. This occurs because when a peak is at the boundary, the total amplitude will be greater than when zeroes are at the boundaries. Thus,

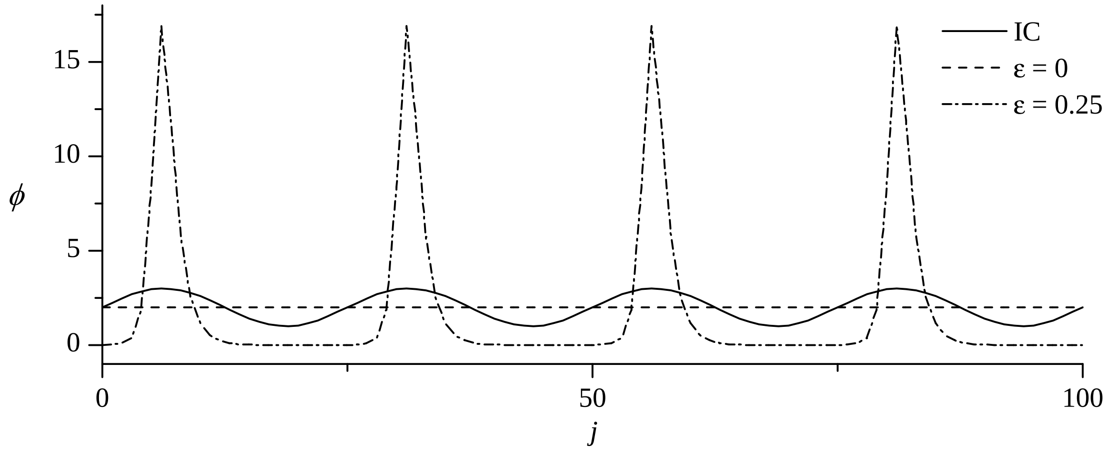

Figure 2.1: Propagation of sinusoidal wave without ($\varepsilon = 0$) and with ($\varepsilon = 0.25$) negative diffusion

the total amplitude behaves periodically after the scheme reaches convergence, which can be seen in Fig. 2.2.

To show that the wave speed is preserved, during a numerical experiment, the time step n that a peak passes at j_0 is recorded. The difference between two consecutive recorded time steps is the period T. Since multiple time steps are recorded, an averaged period, T_{avg}, is obtained. The wave speed is calculated by using Eq. (2.7) and the numerically computed period T_{avg}

$$\sigma = \frac{\lambda_s}{T_{\text{avg}}}. \tag{2.48}$$

σ should be approximately ν. Numerical experiments for different sets of parameters are performed and Table 2.1 provides the results. As expected, the wave speed σ is close to ν.

Varying the Wave Length of the Initial Condition

The initial condition (IC) is given by Eq. (2.41)

$$\phi_j^0 = 2 + \sin\left(\frac{2\pi j}{\lambda_s}\right).$$

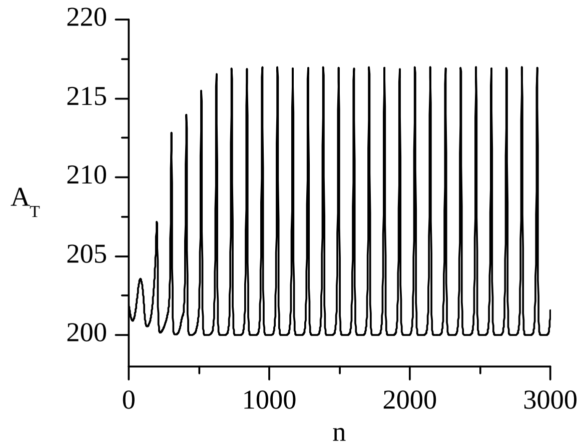

Figure 2.2: Conservation of total amplitude

Table 2.1: Conservation of wave speed

Experiment	λ_s	ν	μ	ε	T_{avg}	$\sigma = \lambda_s/T_{avg}$
I	20	0.23	0.20	0.25	86.97	0.2300
II	25	0.23	0.20	0.25	108.8	0.2297
III	35	0.30	0.20	0.25	108.8	0.2999
IV	40	0.27	0.20	0.30	116.7	0.2699

An analysis of the wave length of the initial condition (λ_s) was done to establish for which frequencies of periodic waves WC can be implemented. All other parameters were fixed at: convection speed, $\nu = 0.23$; dissipation, $\mu = 0.2$; and confinement, $\varepsilon = 0.25$. For these parameters, the results show that when $12 \leq \lambda_s \leq 52$ gridpoints, the converged solution is in accordance with the IC, which means that the number of cycles of IC is the number of hyperbolic secants. Fig. 2.3 shows the propagation for different wave lengths. This proper behavior occurs because each hyperbolic secant has exponential tails that decrease with distance and, if the tail decreases beyond a certain level, it will behave as if there was no overlap and remain as stable pulses.

On the other hand, when $\lambda_s < 12$ gridpoints, λ_s is not large enough for the hyperbolic secants to keep their information, which means the exponential tails

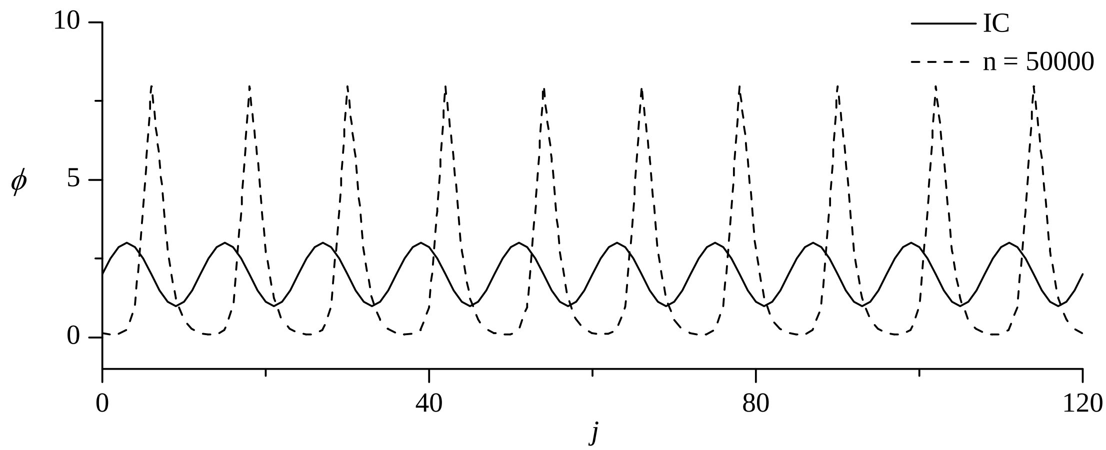

(a) $\lambda_s = 12$

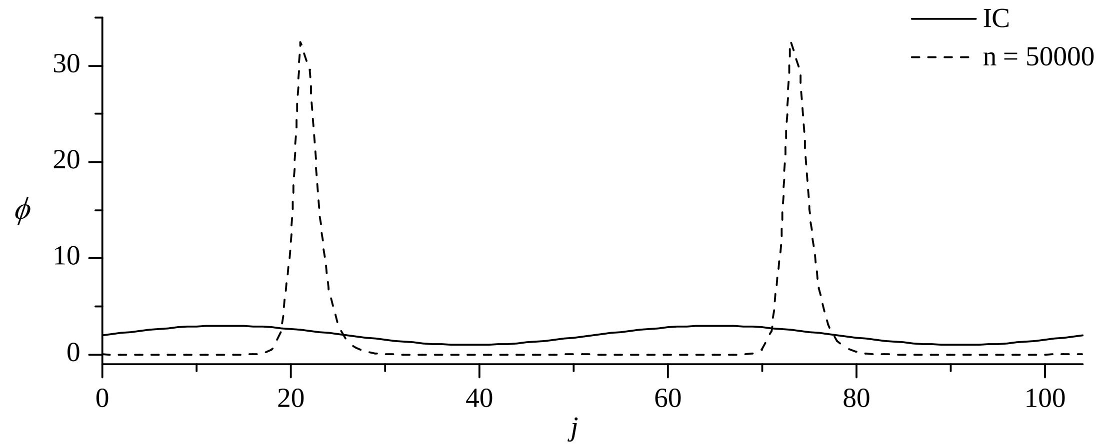

(b) $\lambda_s = 52$

Figure 2.3: Different wave lengths that converge to the proper discrete solution to plottable accuracy

overlap and, consequently, each eventually merges with its adjacent pulses. Because of the merging, the number of initial cycles is not the same as the number of hyperbolic secant as seen in Fig. 2.3. In addition, when $\lambda_s > 52$ gridpoints, the method becomes unstable because the negative diffusion term is insufficient and the solution splits into multiple hyperbolic secant pulses. Thus, instead of having one hyperbolic secant per cycle of IC, the method creates more hyperbolic secants. Fig. 2.4 shows that when λ_s is too large, we have more pulses than expected.

Convection Speed Variation

For this analysis, the value of the convection speed, ν, is varied while other parameters are fixed. The expected value for stability is $0 < \nu \leq 1$ (Anderson et al. (1984)). However, because of the confinement term, ν has a more restricted condition. Our analysis finds that stability depends on the combination of confinement and convection speed. As the values of confinement increase, the upper bound for stable values of convection speed decrease. The adequate procedure is to do numerical trials to assure stability for the combination of parameters. For example, for these values of confinement, $\varepsilon = 0.25$ or $\varepsilon = 0.3$, we need $0 \leq \nu \leq 0.35$.

Confinement Variation

The wave confinement parameter, ε, determines the width of the converged hyperbolic secant. This occurs because γ from Eq.(2.38), which is dependent on ε, defines the width of the hyperbolic secant of Eq.(2.40). Therefore, as ε varies, we should expect to have different widths of the converged solution.

For this analysis, the confinement parameter is varied while the IC and all other parameters are fixed at: IC, $\lambda_s = 20$; convection speed, $\nu = 0.23$; and dissipation $\mu = 0.2$. We found that for $\mu \leq \varepsilon < 2\mu$, we get the expected solution. When $\varepsilon \geq 2\mu$, the method is divergent. When $\varepsilon < \mu$, the method is dissipative. This is explained

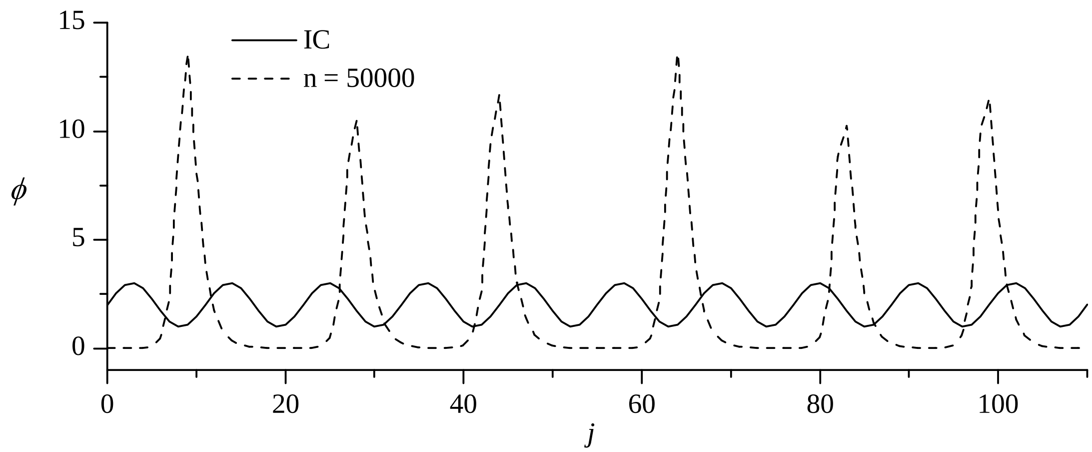

(a) $\lambda_s = 11$

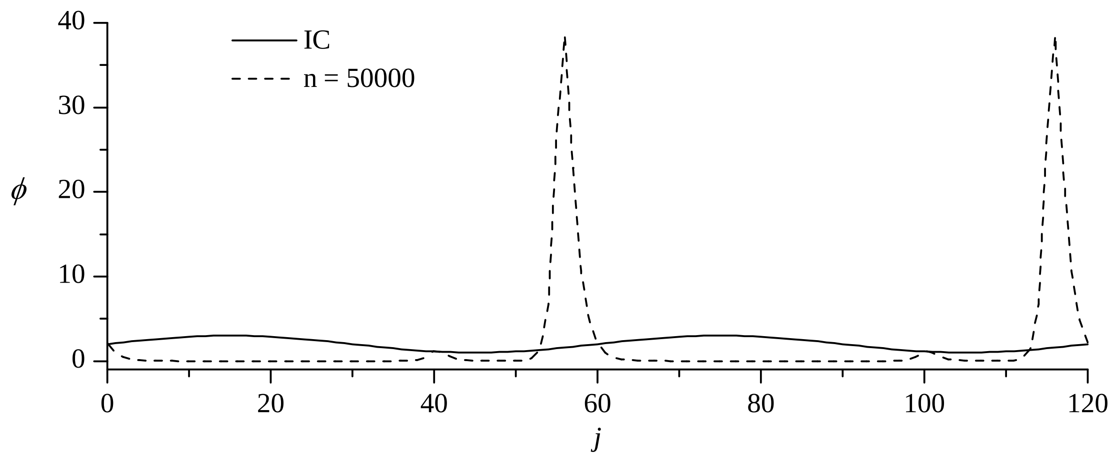

(b) $\lambda_s = 60$

Figure 2.4: Different wave lengths that do not converge to the proper solution

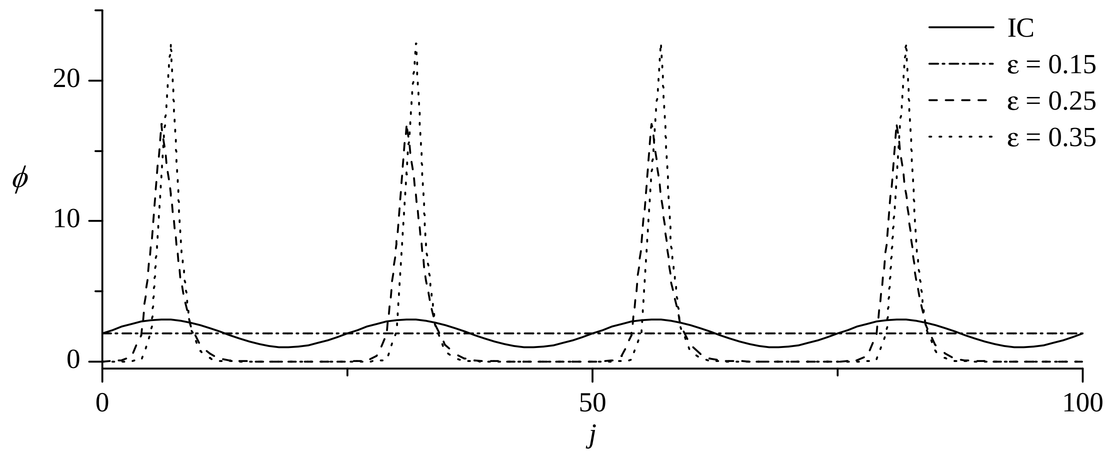

Figure 2.5: IC and converged solutions for different values of confinement, ε

from Eq.(2.37): for γ to be real, we need

$$\frac{3\,\varepsilon}{\mu} - 1 \geq 2 \Rightarrow \varepsilon \geq \mu. \tag{2.49}$$

Therefore,

$$\mu \leq \varepsilon \leq 2\mu. \tag{2.50}$$

The first condition of Eq. (2.50) comes from Eq. (2.49) whereas the second condition comes from numerical experiments. When Eq.(2.50) is satisfied, it is assured that sufficient negative diffusion is added to the system. Otherwise, the method is dissipative and a converged solution is not obtained. Fig. 2.5 shows the converged solution for different values of ε.

Approximation of Analytical Solution

As explained in Section 2.1.2, superposition of the analytical solution (Eq.(2.31)) is not possible due its nonlinearity. However, an approximate analytical solution may be calculated by assuming the overlap of exponential tails of the hyperbolic secants is exponentially small and can be approximated as zero. This approximate solution is derived from the converged solution. After the method reaches convergence in the numerical trial, the program calculates: The number of hyperbolic secants, m, by a simple logic step in the program; γ by Eq. (2.38); and the amplitude of each hyperbolic secant, B, by Eq. (2.44). Then the approximate analytical solution is

- For m even

$$\phi_j^{\text{analytical}} = B \operatorname{sech}\left[\gamma\left(j - j_c \pm k\frac{\lambda}{2}\right)\right], \qquad k = 1, 3, 5, \ldots, m-1 \tag{2.51}$$

- For m odd

$$\phi_j^{\text{analytical}} = B \operatorname{sech}\left[\gamma\left(j - j_c \pm k\lambda\right)\right], \qquad k = 0, 1, 2, 3, \ldots, m/2 \tag{2.52}$$

where j_c is the centroid position defined by

$$j_c = \frac{\sum_{j=0}^{J-1} j\phi_j^N}{A_T}, \tag{2.53}$$

A_T is obtained from Eq. (2.6), and λ is given from the initial condition.

Fig. 2.6 shows the approximate analytical solution for two sets of parameters.

Transformation of Converged Solution Back to Initial Condition

The results shown in Fig. 2.7 were obtained using the procedure described in Section 2.2.3. This final transformation is very important because it means WC can be applied to practical problems.

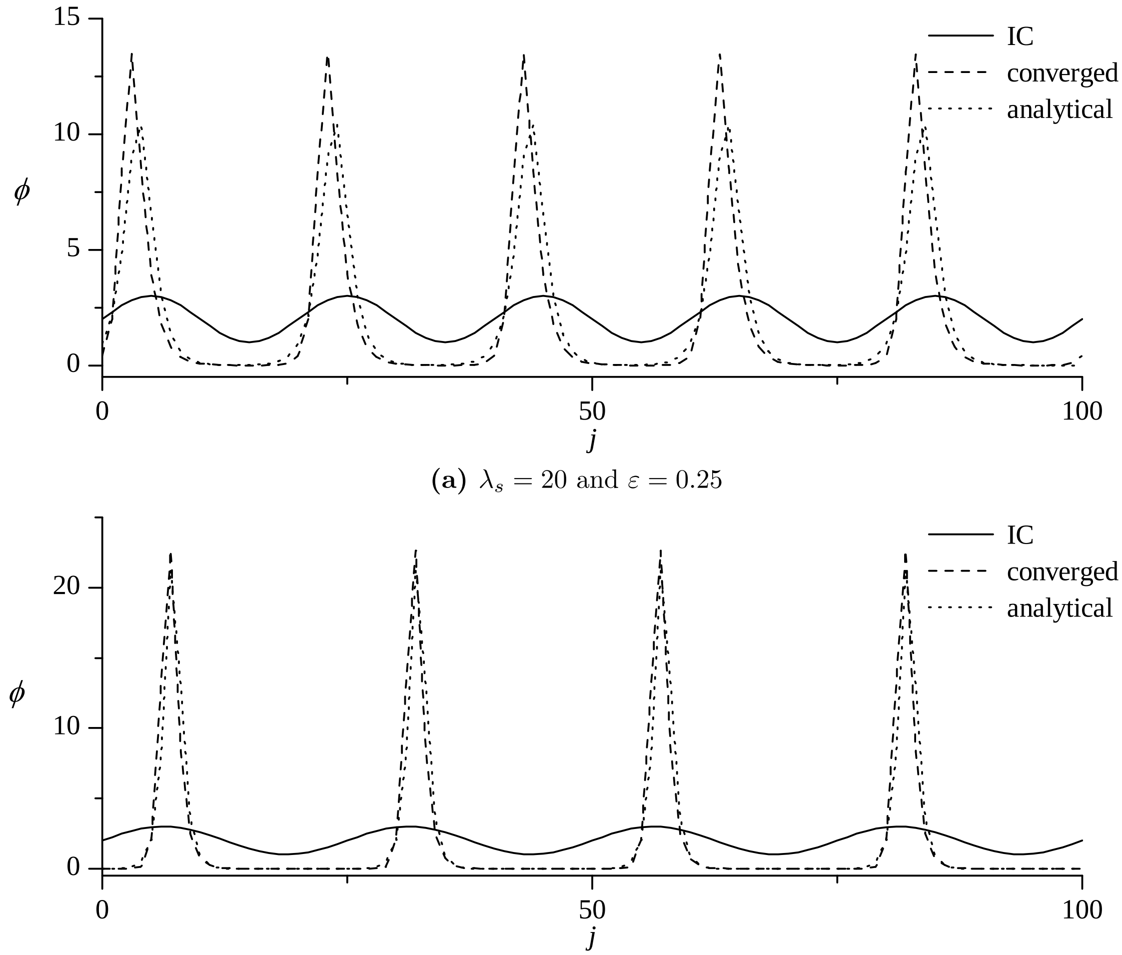

(a) $\lambda_s = 20$ and $\varepsilon = 0.25$

(b) $\lambda_s = 25$ and $\varepsilon = 0.35$

Figure 2.6: Converged solution ($n = 50000$) for different set of parameters ($\nu = 0.23$ and $\mu = 0.2$)

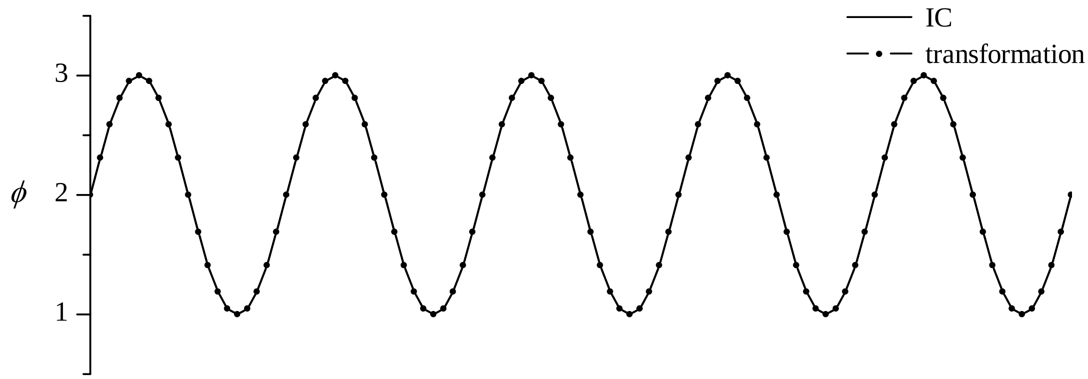

(a) $\lambda_s = 20$ and $\varepsilon = 0.25$

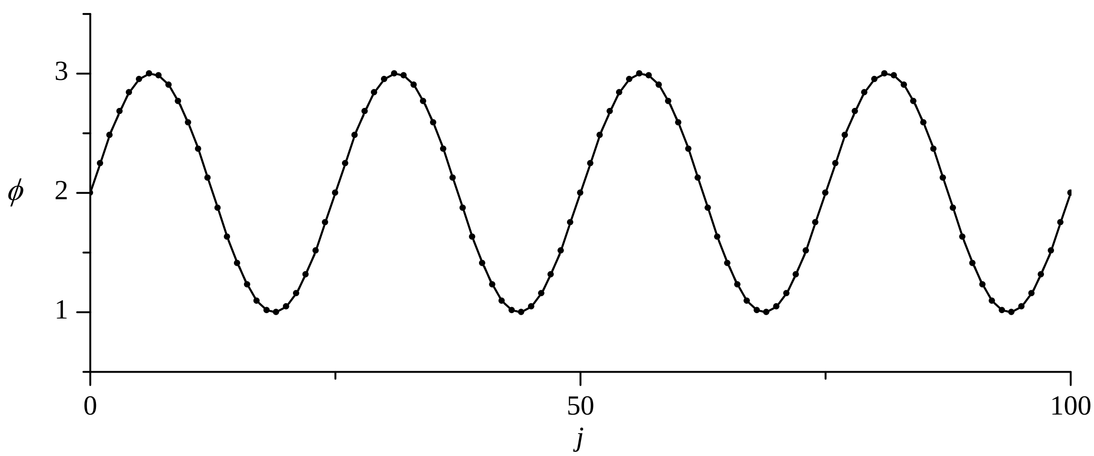

(b) $\lambda_s = 25$ and $\varepsilon = 0.35$

Figure 2.7: Transformation to IC for different set of parameters ($\nu = 0.23$ and $\mu = 0.2$)

2.3 Positive Waves with Varying Amplitude

2.3.1 Numerical Experiment

Discretized Equation

The following discretized equation (Eq. (2.4))

$$\phi_j^{n+1} = \phi_j^n - \frac{\nu}{2}\left(\phi_{j+1}^n - \phi_{j-1}^n\right) + \mu\left(\phi_{j-1}^n - 2\phi_j^n + \phi_{j+1}^n\right) - \varepsilon\left(\Phi_{j-1}^n - 2\Phi_j^n + \Phi_{j+1}^n\right)$$

is used to perform the numerical experiments.

Boundary Conditions

Periodic boundary conditions ($\phi_0^n = \phi_{J-1}^n$) are used for these numerical experiments.

Initial Condition

In order to produce a smooth periodic wave with varying amplitude, the sine function is multiplied by a cosine function

$$\phi_j^0 = \left[2 + \sin\left(\frac{2\pi j}{\lambda_s}\right)\right]\left[0.75 + 0.25\cos\left(\frac{2\pi j}{\lambda_c}\right)\right], \tag{2.54}$$

where the constant 0.75 is added to maintain a positive wave.

2.3.2 Results and Discussion

Initial Condition Variation

The objective of this experiment is to determine if WC is capable of propagating periodic waves with varying amplitude. A cosine function is used to produce a smooth variation in amplitude and numerical experiments are done to determine for which λ_s and λ_c the method is convergent. In order to have more flexibility for λ_c, the grid size was extended to $20\lambda_s + 1$, as opposed to 4 to 5 λ_s previously used. It is found that the method is convergent for

$$\lambda_s \leq \lambda_c < J, \tag{2.55}$$

and the constraint for λ_s is

$$18 \leq \lambda_s \leq 37 \text{ gridpoints.} \tag{2.56}$$

Fig. 2.8 shows the behavior of the period waves with varying amplitude.

2.4 Waves with Varying Signs

2.4.1 Numerical Experiment

Discretized Equation

The following discretized equation (Eq. (2.4))

$$\phi_j^{n+1} = \phi_j^n - \frac{\nu}{2}\left(\phi_{j+1}^n - \phi_{j-1}^n\right) + \mu\left(\phi_{j-1}^n - 2\phi_j^n + \phi_{j+1}^n\right) - \varepsilon\left(\Phi_{j-1}^n - 2\Phi_j^n + \Phi_{j+1}^n\right)$$

is used to perform the numerical experiments.

Boundary Conditions

Periodic boundary ($\phi_0^n = \phi_{J-1}^n$) conditions are used for these numerical experiments.

Initial Condition

In order to produce a periodic wave with varying signs, we use a simple sinusoidal function

$$\phi_j^0 = \sin\left(\frac{2\pi j}{\lambda_s}\right) \tag{2.57}$$

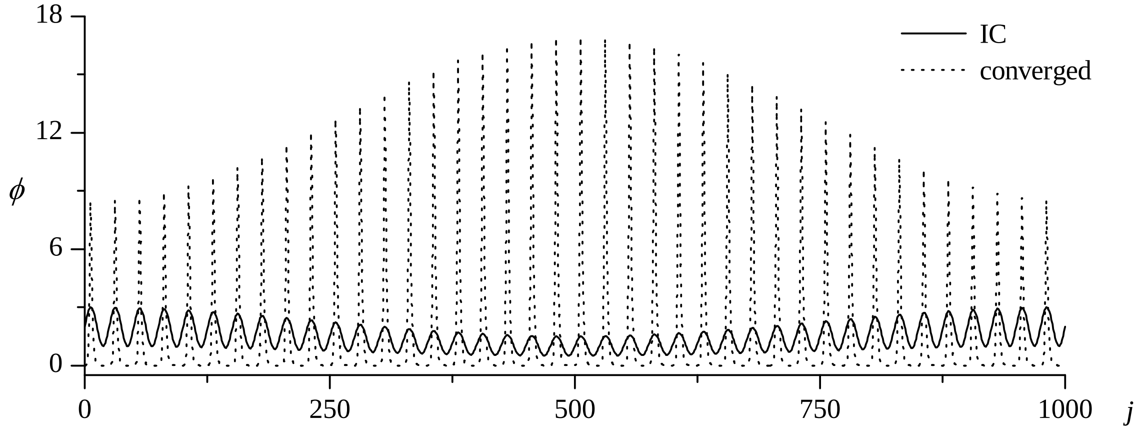

(a) One cycle of cosine function ($\lambda_c = 1000$), $\lambda_s = 25$, and $J = 1001$

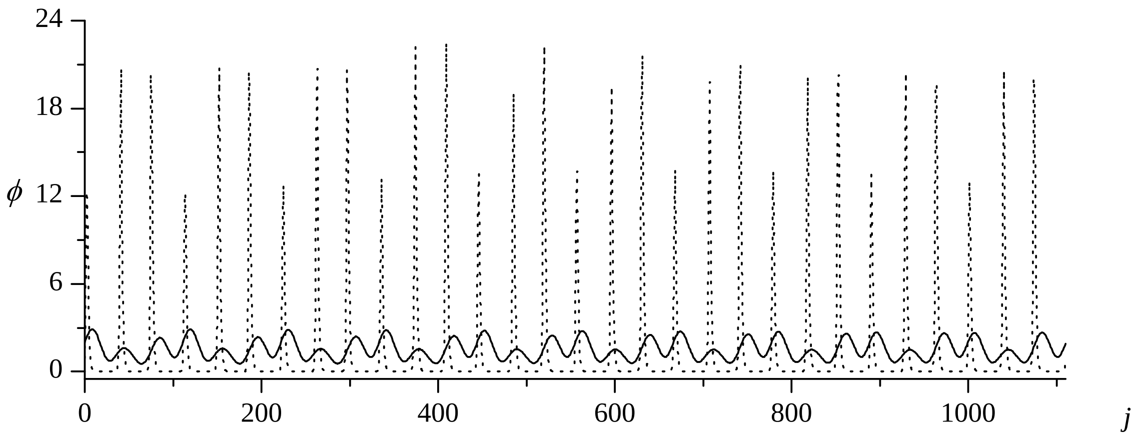

(b) Ten cycles of cosine function ($\lambda_c = 110$), $\lambda_s = 37$, and $J = 1111$

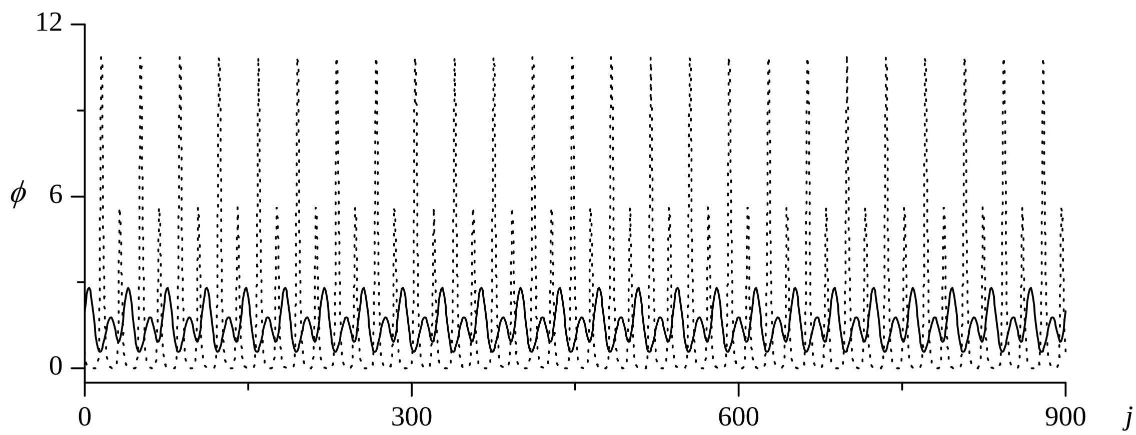

(c) Twenty five cycles of cosine function ($\lambda_c = 36$), $\lambda_s = 18$, and $J = 901$

Figure 2.8: Initial condition and converged solution ($n = 50000$) for different cosine functions with $\nu = 0.23$, $\mu = 0.2$, and $\varepsilon = 0.25$

2.4.2 Results and Discussion

Harmonic Mean Variation

When the scalar that is propagated does not have a single sign, the harmonic mean, Eq. (2.5), has to appropriately handle the different signs. Otherwise, if the original form from Eq. (2.5) is maintained, the method is divergent. Four different forms are tested to determine which one is appropriate.

1. Absolute value with sign function

   The modified harmonic mean is defined as

$$\Phi_j^n = \mathrm{sgn}(\phi_j^n)\frac{3}{\frac{1}{|\phi_{j-1}^n|}+\frac{1}{|\phi_j^n|}+\frac{1}{|\phi_{j+1}^n|}}. \tag{2.58}$$

   The modified harmonic mean with absolute values and sign function keeps the positive part of the sinusoidal wave as a positive hyperbolic secant and the negative part as a negative hyperbolic secant, which is the expected solution.

   The values for the negative diffusion parameter have to be adjusted in order to produce enough negative diffusion. The typical value previously used ($\mu = 0.2$ and $\varepsilon = 0.25$) does not produce enough negative diffusion. Thus, it is attempted to use the ratio established by Chitta (2008)

$$\frac{\varepsilon}{\mu} = 1.5, \tag{2.59}$$

   but the scheme is still dissipative. A new ratio that gives good results is then determined

$$\frac{\varepsilon}{\mu} = 2.0, \tag{2.60}$$

   where $0.12 \le \mu \le 0.2$. Fig. 2.9 shows results for two sets of parameters. The observed total phase shift is extremely small when divided by the number of time steps. However, its origin is of future investigation.

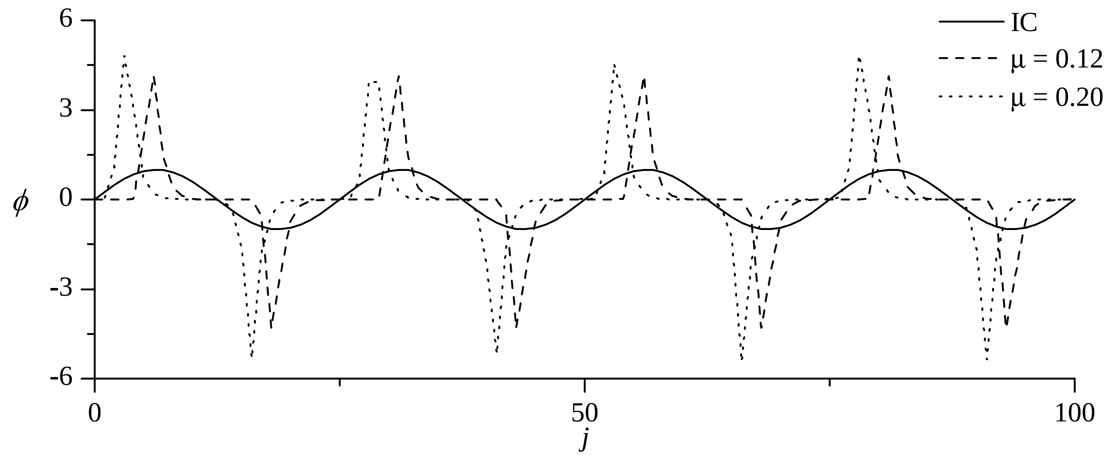

Figure 2.9: Initial condition and converged solution ($n = 50000$) using the modified harmonic mean defined by Eq. (2.58), ratio of ε and μ defined by Eq. (2.60), $\nu = 0.23$, and $\lambda_s = 25$

2. Absolute value without sign function

The modified harmonic mean is defined as

$$\Phi_j^n = \frac{3}{\frac{1}{|\phi_{j-1}^n|} + \frac{1}{|\phi_j^n|} + \frac{1}{|\phi_{j+1}^n|}}. \tag{2.61}$$

When the IC is defined by Eq. (2.57), the modified harmonic mean with absolute values but no sign function produces a dissipative scheme regardless of the ε and μ values. Because the harmonic mean is always positive, it adds negative diffusion to the positive part of the wave but also adds negative diffusion to the negative part of the wave. This means that the negative part is diffusive and eventually will average out the positive values.

However, when a small positive value is added to the initial condition, for example

$$\phi_j^0 = 0.5 + \sin\left(\frac{2\pi x}{\lambda_s}\right), \tag{2.62}$$

then the method is convergent. This occurs because there is not enough negative amplitude to balance out the positive values. But when a negative value is added, the method is dissipative – for the same reason explained above – and converges to the average value of the sinusoidal function. For example, if the constant added is -0.5, the method converges to a constant function of -0.5. Fig. 2.10 shows the behavior of the harmonic mean defined by Eq. (2.61) for different IC. Again, the origin of the small phase shift will be explored.

3. Square root with sign function

   The modified harmonic mean is defined as

$$\Phi_j^n = \operatorname{sgn}(\phi_j^n)\left[\frac{3}{\frac{1}{(\phi_{j-1}^n)^2}+\frac{1}{(\phi_j^n)^2}+\frac{1}{(\phi_{j+1}^n)^2}}\right]^{\frac{1}{2}}. \tag{2.63}$$

   The square root of the modified harmonic mean with the sign function produces the similar results as the modified harmonic mean defined by Eq. (2.58), but the parameters must be adjusted accordingly. For this modified harmonic mean, the ratio defined by Eq. (2.60) does not suffice. A new ratio is determined

$$\frac{\varepsilon}{\mu} = 2.25, \tag{2.64}$$

   where $0.12 \leq \mu \leq 0.2$.

   Fig. 2.11 shows the similar behavior between Eq. (2.63) and Eq. (2.58). Again, the positive parts of the sinusoidal wave become positive hyperbolic secants whereas the negative parts become negative hyperbolic secants.

4. Square root without sign function

   The modified harmonic mean is defined as

$$\Phi_j^n = \left[\frac{3}{\frac{1}{(\phi_{j-1}^n)^2}+\frac{1}{(\phi_j^n)^2}+\frac{1}{(\phi_{j+1}^n)^2}}\right]^{\frac{1}{2}}. \tag{2.65}$$

   The square root of the modified harmonic mean without the sign function produces the similar results as the modified harmonic mean defined by Eq.

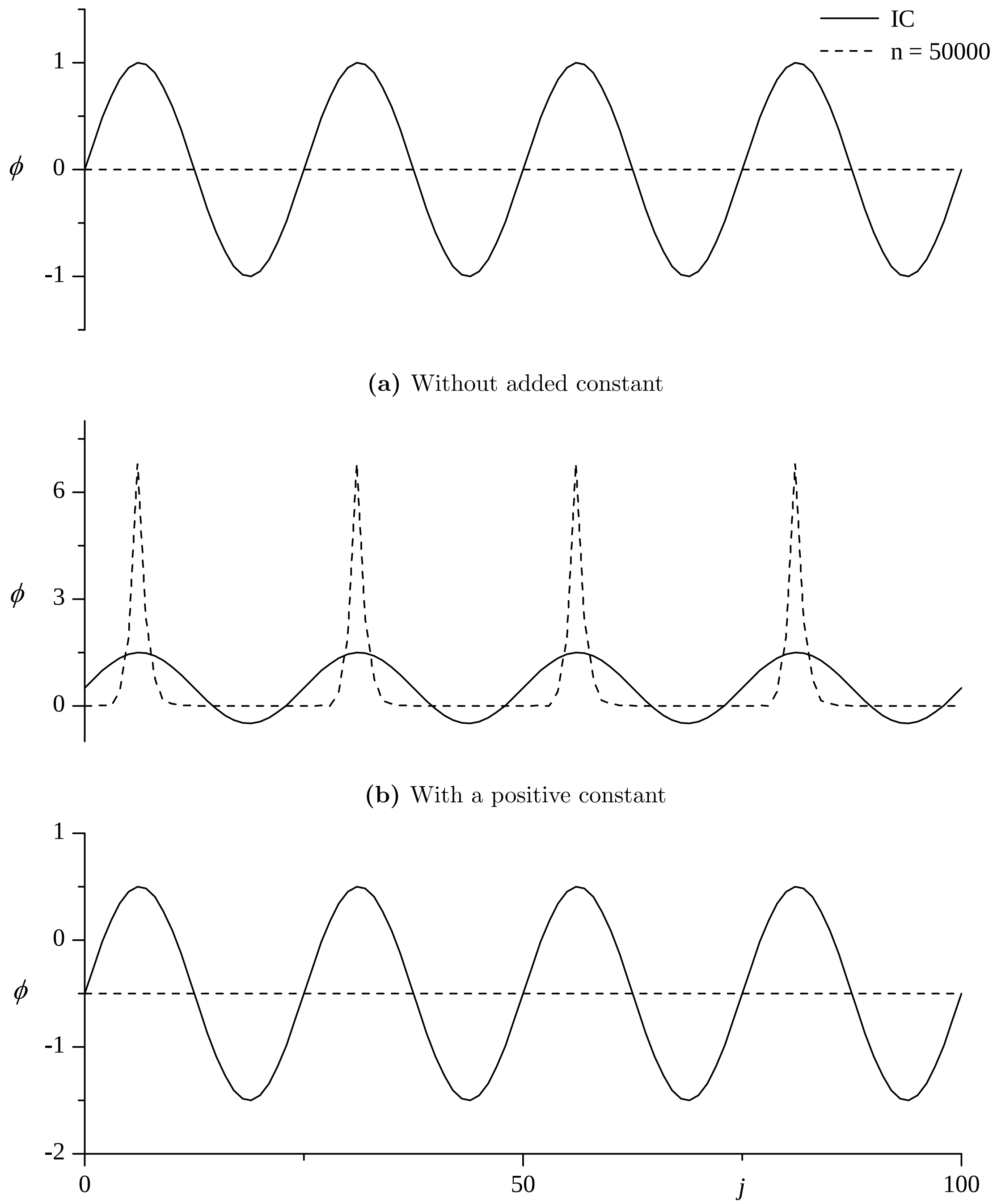

(a) Without added constant

(b) With a positive constant

(c) With a negative constant

Figure 2.10: Propagation of sinusoidal wave with harmonic mean defined by Eq. (2.61), $\lambda_s = 20$, $\nu = 0.23$, $\mu = 0.2$, and $\varepsilon = 0.25$

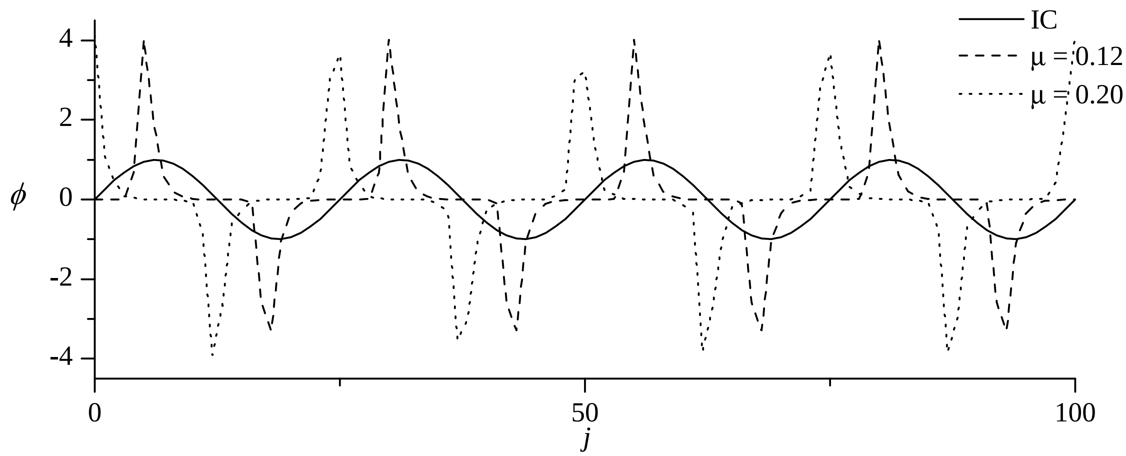

Figure 2.11: Initial condition and converged solution ($n = 50000$) using harmonic mean defined by Eq. (2.63), ratio of ε and μ defined by Eq. (2.64), $\nu = 0.23$, and $\lambda_s = 25$

(2.61), but the ratio used for ε and μ is from Eq. (2.64). As encountered for Eq. (2.61), the convergence of Eq. (2.65) depends on the constant that is added to the IC. For a positive constant, the method converges to a series of hyperbolic secants and for a negative constant, it converges to the value of the constant.

Chapter 3

Wave Equation

The previous chapter has an extensive study of wave confinement (WC) for the one-dimensional (1D) advection equation. As a continuation of this investigation, WC is implemented for the 1D wave equation. First, a formulation of the numerical scheme is presented. Then, numerical tests are performed for the different cases: positive waves with constant amplitude, positive waves with varying amplitude, and waves with varying signs.

3.1 Formulation

The wave equation

$$\frac{\partial^2 \phi}{\partial t^2} - c^2 \frac{\partial^2 \phi}{\partial x^2} = 0 \tag{3.1}$$

may be discretized into

$$\frac{\phi_j^{n+1} - 2\phi_j^n + \phi_j^{n-1}}{(\Delta t)^2} = c^2 \, \frac{\phi_{j+1}^n - 2\phi_j^n + \phi_{j-1}^n}{h^2}. \tag{3.2}$$

WC adds a nonlinear term E_2 to Eq. (3.2)

$$\phi_j^{n+1} = 2\phi_j^n - \phi_j^{n-1} + \frac{c^2(\Delta t)^2}{h^2} \left(\phi_{j+1}^n - 2\phi_j^n + \phi_{j-1}^n \right) + E_2, \tag{3.3}$$

where E_2 is

$$E_2 = \delta_n \delta_j^2 F = \delta_n \delta_j^2 (\mu \phi_j^n - \varepsilon\, \Phi_j^n) \tag{3.4}$$

where Φ is defined by Eq. (2.5). Then the fully discretized equation is

$$\begin{aligned}
\phi_j^{n+1} =& 2\phi_j^n - \phi_j^{n-1} \\
&+ \nu^2 \left(\phi_{j+1}^n - 2\phi_j^n + \phi_{j-1}^n\right) \\
&+ \mu \left(\phi_{j+1}^n - 2\phi_j^n + \phi_{j-1}^n\right) - \varepsilon \left(\Phi_{j-1}^n - 2\Phi_j^n + \Phi_{j+1}^n\right) \\
&- \mu \left(\phi_{j+1}^{n-1} - 2\phi_j^{n-1} + \phi_{j-1}^{n-1}\right) + \varepsilon \left(\Phi_{j-1}^{n-1} - 2\Phi_j^{n-1} + \Phi_{j+1}^{n-1}\right)
\end{aligned} \tag{3.5}$$

3.2 Positive Waves with Constant Amplitude

3.2.1 Numerical Experiment

Discretized Equation

Eq. (3.5) is used to perform the numerical experiments.

Boundary Conditions

Periodic boundary conditions ($\phi_0^n = \phi_{J-1}^n$) are used for these numerical experiments.

Initial Condition

The initial condition is

$$\phi_j^0 = \phi_j^1 = \begin{cases} 2 + \sin\left(\frac{2\pi j}{\lambda_s}\right), & 5\lambda_s \leq j \leq 15\lambda_s \\ 2, & \text{otherwise} \end{cases} \tag{3.6}$$

and $J = 20\lambda_s + 1$.

3.2.2 Results and Discussion

Unlike for a single pulse – where the scalar quantity can go through many interactions – there appears to be an error build-up when the sine waves go through each other (for periodic boundary conditions). This is due to the discontinuity in the slope where the function transitions from a constant to a sinusoidal wave. At this discontinuity, when the waves collide, an error builds up. This error build-up can be avoided by extending the grid size, which excludes collisions. Or for the case where collisions do happen and where this slope discontinuity must be included, the error build up can be overcome by setting

$$\frac{\varepsilon}{\mu} = 1.025 \tag{3.7}$$

more specifically, $\mu = 0.2$ and $\varepsilon = 0.205$, which is different than the ratios previously used from Eq.'s (2.59, 2.60, 2.64). The present case appears to be an isolated value, which is different from the continuous waves that can be propagated and collided with minimal error for a range of ε/μ. For this discontinuous case, the method is very sensitive to changes in the values of the parameters. For instance, if $\varepsilon = 0.2$, the method is dissipative and if $\varepsilon = 0.21$, the method has an error build-up.

Initial Condition Variation

The objective of these trials is to determine for which range of λ_s WC works. All other parameters were fixed at $\nu = 0.23$, $\mu = 0.2$, $\varepsilon = 0.205$, and $J = 20\lambda_s$. When $\lambda_s \leq 22$ gridpoints, the method does not converge to the proper solution. An upper bound for λ_s is not determined, but it is found that the method converges for λ_s as long as 500 gridpoints. Thus, the condition for λ_s is

$$\lambda_s \geq 23 \ \text{ gridpoints.} \tag{3.8}$$

Fig. 3.1 shows the propagation and interaction of a sinusoidal wave.

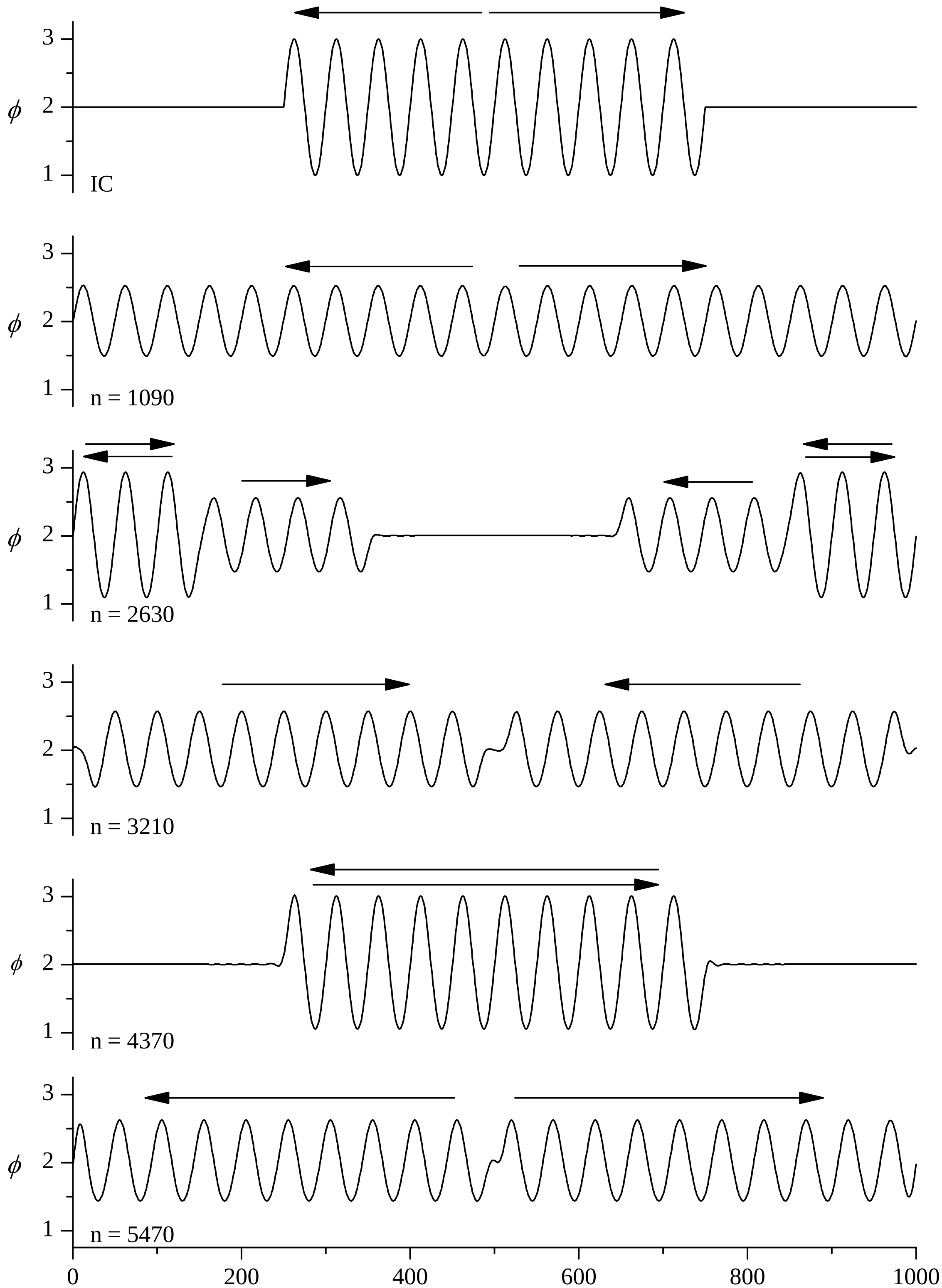

Figure 3.1: Propagation and interaction of sinusoidal wave with $\lambda_s = 50$, $\nu = 0.23$, $\mu = 0.2$, and $\varepsilon = 0.205$

3.3 Positive Waves with Varying Amplitude

3.3.1 Numerical Experiment

Discretized Equation

Eq. (3.5) is used to perform the numerical experiments.

Boundary Conditions

Periodic boundary conditions ($\phi_0^n = \phi_{J-1}^n$) are used for these numerical experiments.

Initial Condition

The initial condition is

$$\phi_j^0 = \phi_j^1 = \begin{cases} \left[2 + \sin\left(\frac{2\pi j}{\lambda_s}\right)\right]\left[b + 0.25\cos\left(\frac{2\pi j}{\lambda_c}\right)\right], & 5\lambda_s \leq j \leq 15\lambda_s \\ 2, & \text{otherwise} \end{cases} \tag{3.9}$$

where $\lambda_c = a\lambda_s$ such that a is a positive integer constant, $J = 20\lambda_s + 1$, and b is a positive constant that needs to be adjusted in a way that it does not create a jump between the points where the functions change (e.g. from $5\lambda_s - 1$ to $5\lambda_s$ and from $15\lambda_s$ to $15\lambda_s + 1$).

3.3.2 Results and Discussion

Again, for these numerical trials, the ratio for ε and μ is defined by Eq. (3.7).

Initial Condition Variation

The objective of this experiment is to determine if WC is capable of propagating periodic waves with varying amplitude. As in the previous chapter, a cosine function is used to produce the variation in amplitude. It is important to establish for which λ_s and λ_c the method converges. Numerical experiments show that the method is convergent for

$$\lambda_s \leq \lambda_c \leq 10\lambda_s \tag{3.10}$$

where $\lambda_s \geq 23$ gridpoints.

Fig. 3.2 shows the propagation and interaction of a periodic wave with varying amplitude.

3.4 Waves with Varying Signs

3.4.1 Numerical Experiment

Discretized Equation

Eq. (3.5) is used to perform the numerical experiments reported in this section.

Boundary Conditions

Periodic boundary conditions ($\phi_0^n = \phi_{J-1}^n$) are used for these numerical experiments.

Initial Condition

The initial condition is

$$\phi_j^0 = \phi_j^1 = \begin{cases} \sin\left(\frac{2\pi j}{\lambda_s}\right), & 5\lambda_s \leq j \leq 15\lambda_s \\ 0, & \text{otherwise} \end{cases} \tag{3.11}$$

and $J = 20\lambda_s + 1$.

3.4.2 Results and Discussion

Again, for these numerical trials, the ratio for ε and μ is defined by Eq. (3.7).

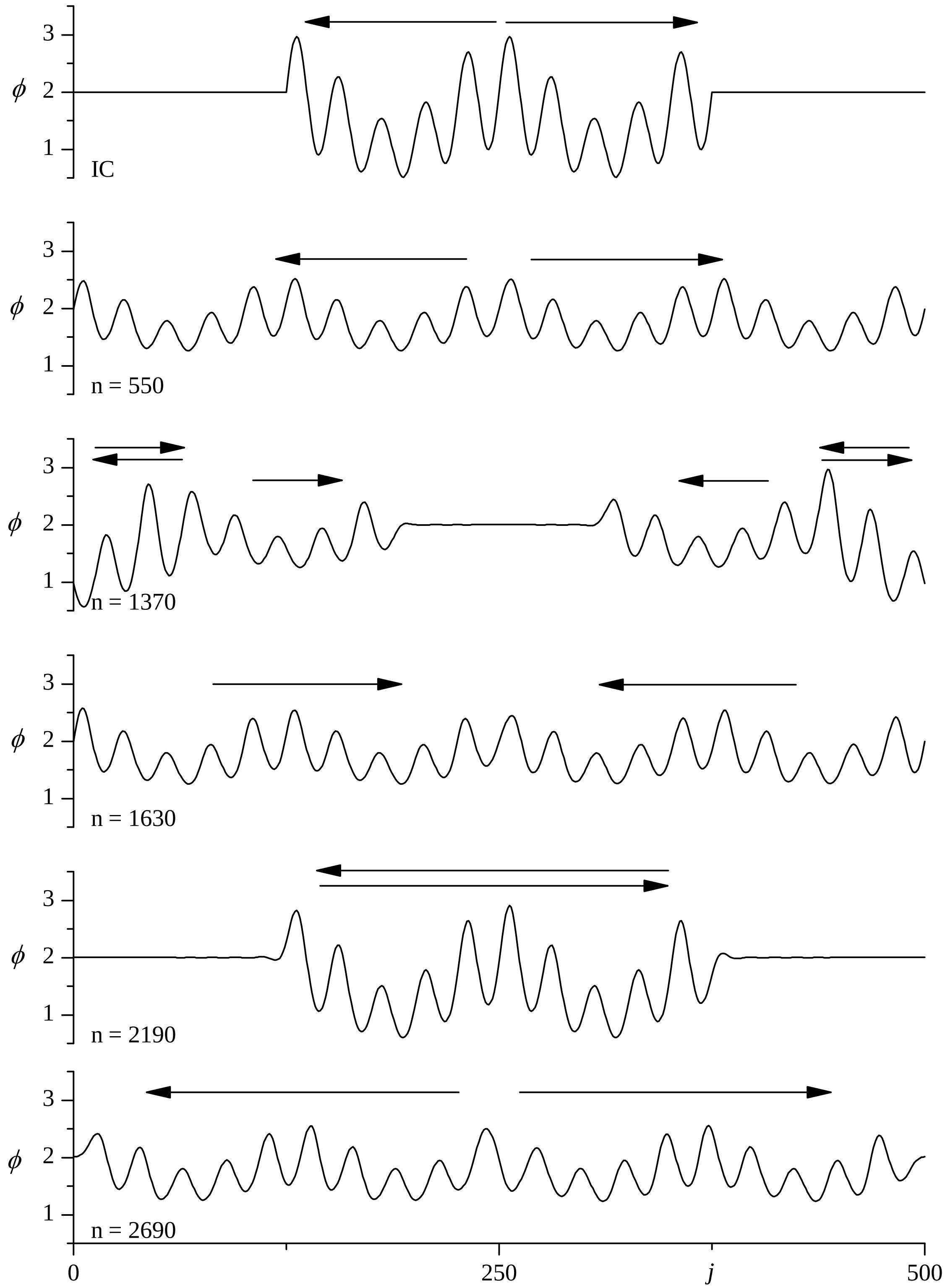

Figure 3.2: Propagation and interaction of periodic wave with varying amplitude and $\lambda_s = 25$, $\lambda_c = 125$, $b = 0.75$, $\nu = 0.23$, $\mu = 0.2$, and $\varepsilon = 0.205$

Harmonic Mean

As in Section 2.4.2, it is attempted to propagate a wave with varying signs, but, for this case, the wave equation is used. Again, the harmonic mean from Eq. 2.5 cannot be used. For the trials in the present section, the harmonic mean defined by Eq. 2.58 is used.

It is found that WC is more sensitive when propagating waves with varying signs than all the other experiments presented here. For values λ_s similar to those previously used (e.g $\lambda_s = 25$ gridpoints), WC is unstable. For this case, an upper bound for λ_s is also found. The constraint is determined to be

$$40 \leq \lambda_s \leq 200 \text{ gridpoints.} \tag{3.12}$$

Unlike positive waves that retain their sinusoidal shape, WC converges waves with varying signs to a hyperbolic secant shape. Fig. 3.3 shows the hyperbolic secant shape of a converged solution.

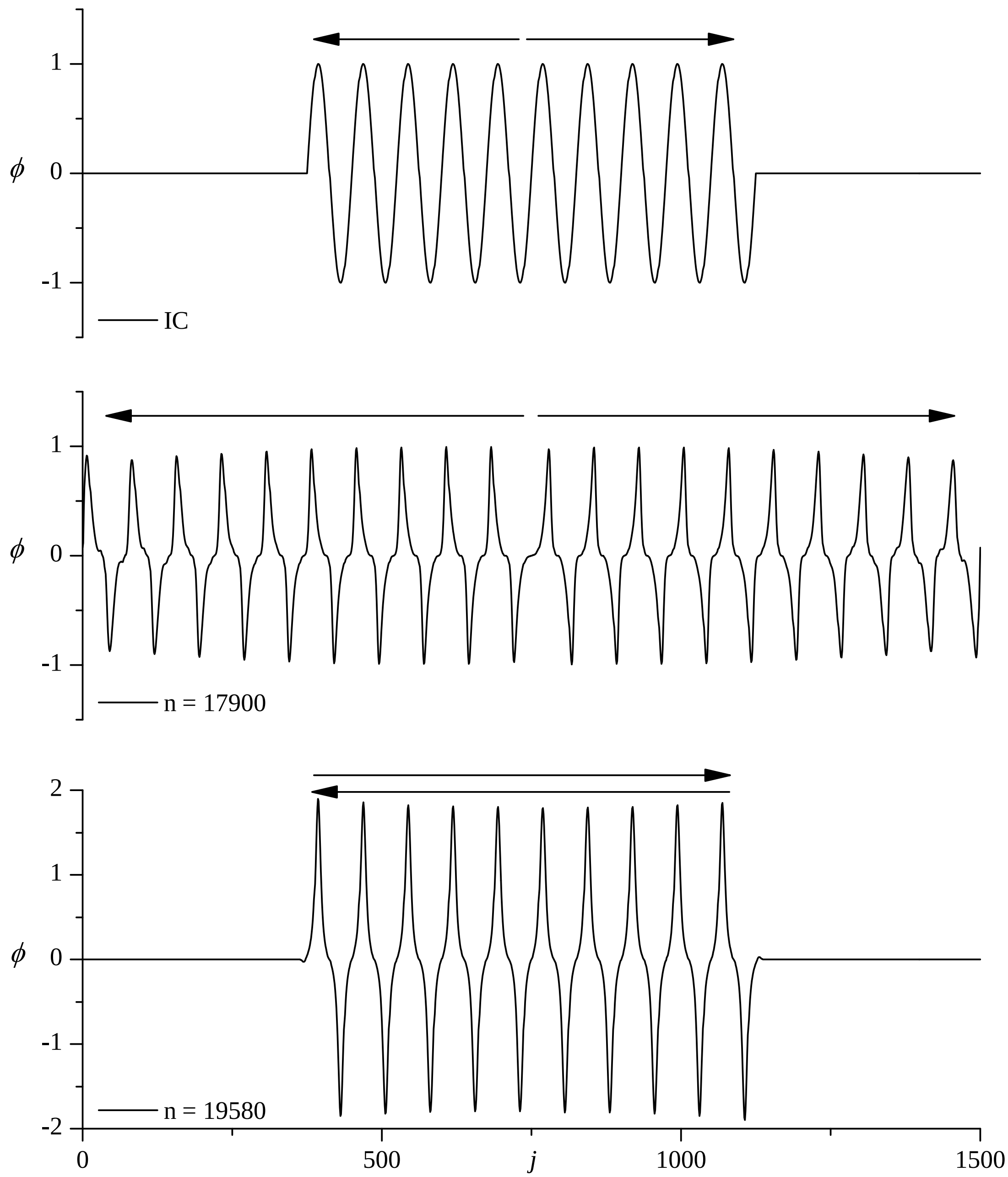

Figure 3.3: Propagation and interaction of periodic wave with varying signs and $\lambda_s = 75$, $\nu = 0.23$, $\mu = 0.2$, and $\varepsilon = 0.205$

Chapter 4

Conclusion

Wave confinement (WC) successfully propagates periodic waves with both advection and wave equations with no accumulating numerical dissipation.

For the advection equation, WC can propagate single-signed periodic waves with constant and varying amplitude and waves with varying signs. Constraints for the wave length of the initial condition (IC) and the ratio of ε and μ need to be obeyed to obtain convergence. When propagating waves with varying signs, it is important to notice the different ratio of ε and μ.

For the wave equation, WC can also propagate positive waves with constant and varying amplitude and waves with varying signs. The wave equation case, in general, requires more strict constraints than the advection equation case (e.g. the ratio of ε and μ must be very close to 1.025, otherwise the solution diverges or dissipates). This does not apply, however, for the wave length (λ_s) of the IC. One important feature of the wave equation is that, for positive periodic waves, the converged solution is not a series of hyperbolic secants: The converged solution retains its sinusoidal shape (this behavior is not seen for the periodic waves with varying signs).

Results of this thesis clearly show that WC can be used not only to propagate pulses and surfaces, but also periodic waves, which has never been shown before.

Applications for WC are numerous, some examples are radio wave propagation, satellite and cell phone communication, which use electromagnetic waves that are described by the wave equation and, therefore, can be simulated by WC. Another important application is target detection. This is possible because WC is capable of producing the reflective behaviors that occur in the process of target detection.

Future research with WC include comparisons with experiments and other numerical methods, inclusion of other phenomena (e.g. reflection, diffraction, refraction, etc.) and extension of periodic waves to 2 and 3 dimensions.

Bibliography

Bibliography

Anderson, D., Tannehill, J., and Pletcher, R. (1984). *Computational fluid mechanics and heat transfer*. Hemisphere New York.

Chitta, S. (2008). *Nonlinear Localized Dissipative Structures for Long-Time Solution of Wave Equation*. PhD dissertation, The University of Tennessee, Knoxville, Department of Mechanical, Aerospace and Biomedical Engineering.

d'Alembert, J. R. (1747). Investigation of the curve formed by a vibrating string. *Acoustics: Historical and Philosophical Development*, pages 119–123.

Jameson, L. (2000). High order schemes for resolving waves: Number of points per wavelength. *Journal of Scientific Computing*, 15(4):417–439.

Jameson, L. (2003). AMR vs high order schemes. *Journal of Scientific Computing*, 18(1):1–24.

Jiang, G. and Shu, C. (1996). Efficient implementation of weighted ENO schemes. *Journal of Computational Physics*, 126(1):202–228.

Lax, P. (1973). *Hyperbolic systems of conservation laws and the mathematical theory of shock waves*. Society for Industrial Mathematics.

Osher, S. (2008). A Level Set Based Geometrical Eulerian Approach to Computing High Frequency Radar Cross Sections and Multiphase Semiclassical Limits of the Schrodinger Equation. Final report for afosr grant no. fa9550-04-1-0143, Level Set Systems Inc., Pacific Palisades, CA.

Quarteroni, A., Sacco, R., and Saleri, F. (2007). *Numerical mathematics*. Springer Verlag.

Rawlinson, N., Hauser, J., and Sambridge, M. (2008). Seismic ray tracing and wavefront tracking in laterally heterogeneous media. *Advances in geophysics*, 49:203.

Steinhoff, J. and Chitta, S. (2009a). Long distance wave computation using nonlinear solitary waves. unpublished.

Steinhoff, J. and Chitta, S. (2009b). Long range numerical simulation of short waves as nonlinear solitary waves. *Mathematics and Computers in Simulation*, 80(4):752–762.

Steinhoff, J. and Chitta, S. (2009c). Long-time solution of the wave equation using nonlinear dissipative structures. *Integral Methods in Science and Engineering, Volume 2*, pages 339–349.

Vinje, V., Iversen, E., and Gjoystdal, H. (1993). Traveltime and amplitude estimation using wavefront construction. *Geophysics*, 58(8):1157–1166.

Vita

I am originally from São Paulo, Brazil. I came to the United States in 2004 to pursue a Bachelor's degree at Siena Heights University in Adrian, MI. I graduated in 2007 with a Bachelor of Science degree in Applied Mathematics and a Bachelor of Arts degree in Computer and Information Systems. I joined the University of Tennessee Space Institute (UTSI) in 2008 to pursue a Master's degree in Mathematics. I plan to continue my education here at UTSI and obtain a Ph.D. in Engineering Science.